

Understanding and Mitigating Overfitting in Prompt Tuning for Vision-Language Models

Chengcheng Ma*, Yang Liu, Jiankang Deng, *Student Member, IEEE*, Lingxi Xie,
Weiming Dong†, *Member, IEEE*, Changsheng Xu, *Fellow, IEEE*

arXiv:2211.02219v2 [cs.CV] 14 Nov 2022

Abstract—Pre-trained Vision-Language Models (VLMs) such as CLIP have shown impressive generalization capability in downstream vision tasks with appropriate text prompts. Instead of designing prompts manually, Context Optimization (CoOp) has been recently proposed to learn continuous prompts using task-specific training data. Despite the performance improvements on downstream tasks, several studies have reported that CoOp suffers from the overfitting issue in two aspects: (i) the test accuracy on base classes first gets better and then gets worse during training; (ii) the test accuracy on novel classes keeps decreasing. However, none of the existing studies can understand and mitigate such overfitting problem effectively. In this paper, we first explore the cause of overfitting by analyzing the gradient flow. Comparative experiments reveal that CoOp favors generalizable and spurious features in the early and later training stages respectively, leading to the non-overfitting and overfitting phenomenon. Given those observations, we propose Subspace Prompt Tuning (*SubPT*) to project the gradients in back-propagation onto the low-rank subspace spanned by the early-stage gradient flow eigenvectors during the entire training process, and successfully eliminate the overfitting problem. Besides, we equip CoOp with Novel Feature Learner (NFL) to enhance the generalization ability of the learned prompts onto novel categories beyond the training set, needless of image training data. Extensive experiments on 11 classification datasets demonstrate that *SubPT+NFL* consistently boost the performance of CoOp and outperform the state-of-the-art approach CoCoOp. Experiments on more challenging vision downstream tasks including open-vocabulary object detection and zero-shot semantic segmentation also verify the effectiveness of the proposed method. Codes can be found at <https://tinyurl.com/mpe64f89>.

Index Terms—Vision-language model, prompt tuning, overfitting, subspace learning, gradient projection.

I. INTRODUCTION

WITH the recent advances in vision-language pre-training, such as CLIP [1] and ALIGN [2], there has been a growing interest in developing multi-modal foundation models for downstream tasks [3]–[6]. These vision-language models (VLMs) are pre-trained on millions of image-text data pairs to align the vision and language modalities in the same feature space, so the resulting models can obtain impressive performances on downstream tasks in a zero-shot manner with

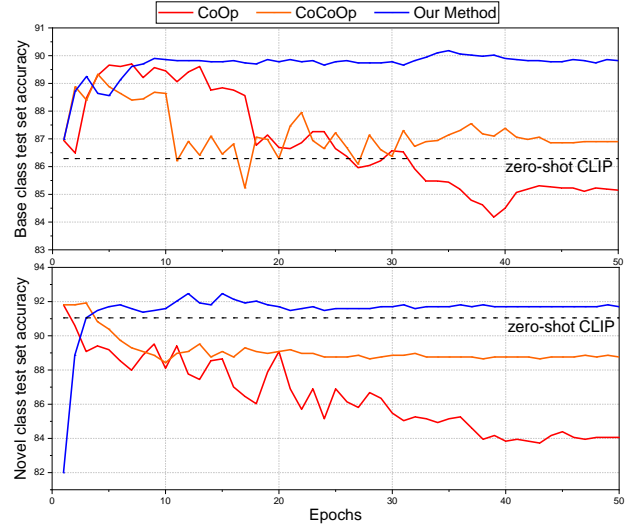


Fig. 1. **Illustrations on two aspects of the overfitting issue in CoOp and CoCoOp.** The dataset is Caltech101. (a) **Up:** The test accuracy on base classes first gets better and then gets worse during the training processes of CoOp and CoCoOp. (b) **Down:** The test accuracy on novel classes keeps decreasing and become far below that of the zero-shot CLIP. Our proposed *SubPT* and NFL can successfully mitigate the overfitting problem.

a properly designed text prompt only, instead of any task-related training data. Early works such as [1] and [2] adopt handcrafted prompt templates like “a photo of a [CLASS]”, which are usually lack of task-specific heuristics and non-robust across different target domains. Inspired by the recent works in the NLP community [7], [8], Zhou *et al.* [9] propose a prompt tuning method named Context Optimization (CoOp) to address such problem, where the prompt can be optimized in a continuous space. CoOp can learn machine-favorable prompts and significantly improve CLIP’s performance on the classification task compared with handcrafted prompts.

Though effective, some recent studies such as [10]–[13] report that CoOp suffers from the overfitting issue in two aspects. First, Zhu *et al.* [11] observe that the test accuracy on base classes first gets better and then gets worse during training, and heavily drops by at most 4% when training ends. We also observe such common failure across many datasets in our experiments (see Fig. 1(a) for an example). Second, Zhou *et al.* [10] notice that the learned prompt is not applicable to novel classes beyond the training set, indicating that CoOp hurts the generalization capability of CLIP. As displayed in Fig. 1(b), the test accuracy on novel classes keeps decreasing during training, far below that of zero-shot CLIP baseline with

*This work was done during an internship in Huawei Inc.

Chengcheng Ma, Weiming Dong, and Changsheng Xu are with National Lab of Pattern Recognition (NLPR), Institute of Automation, Chinese Academy of Sciences (CASIA), Beijing, 100190, China.

Chengcheng Ma is also with School of Artificial Intelligence, University of Chinese Academy of Sciences (UCAS), Beijing, 100049, China.

Yang Liu is with Alibaba DAMO Academy, Hangzhou, 310024, China.

JianKang Deng and Lingxi Xie are with Huawei Inc., Shenzhen 518129, China.

†Corresponding author (weiming.dong@ia.ac.cn).

the handcrafted prompt.

Unfortunately, none of the existing works can effectively mitigate the overfitting problem in CoOp. For instance, Zhou *et al.* [10] introduce Conditional CoOp (CoCoOp) and design image-specific prompts by adding the prompt embedding with MLP-transformed image features. However, as shown in Figs. 1(a) and (b), CoCoOp [10] still fails to prevent base class test set accuracy from decreasing in the later training stage, and the novel class test accuracy is still below that of zero-shot CLIP baseline. Besides, we notice that the conventional anti-overfitting strategies, *e.g.*, early stopping and data augmentation do not work in CoOp. Concretely, CoOp is based on few-shot setting, thus it is unrealistic to collect a validation set for applying early stopping, and data augmentation is not always robust across various downstream datasets and tasks. Also, there is no clue of overfitting when monitoring the entire training process, since the accuracy/loss on training set always keeps increasing/decreasing. To this end, it is important to first understand the cause of overfitting then address the problem accordingly.

In this paper, we first manage to understand the cause of overfitting in CoOp. According to the no free lunch theorem [14], [15], an intuitive understanding is that CoOp favors the generalizable/spurious feature in the early/later training stage, leading to an increase/decrease on the test set accuracy. To investigate the learned features, we measure the gradient flows in early and later training stages, and utilize the dominant eigenvectors of the corresponding checkpoint trajectories to approximate the gradient flow for computational convenience. We observe the same phenomenon across several datasets simultaneously that the two eigenvectors representing early-stage and later-stage gradient flows are almost orthogonal, revealing that CoOp does favor different feature directions in different training stages. To further identify the effects of these two feature directions, we conduct comparative experiments to re-run CoOp from the same initial point, and project the gradients in back-propagation onto the subspace spanned by the early-stage and later-stage eigenvectors respectively during the whole training process. The large performance gap demonstrates that CoOp indeed favors the generalizable/spurious feature in the early/later training stage.

Based on the above observations, we propose Subspace Prompt Tuning (*SubPT*) to mitigate the overfitting problem in prompt tuning. In particular, we first conduct CoOp and collect the saved checkpoints within early training stage to compute the dominate eigenvectors. Then we re-run CoOp from the same initial point and project the gradients onto the subspace spanned by the pre-computed early-stage eigenvectors during the entire training process. The rationale behind *SubPT* lies that the spurious components in gradients can be eliminated during the multiplication process since they are orthogonal to the early-stage gradient flow. Besides, we design Novel Feature Learner (NFL) to enhance the generalization capability towards novel classes without any image training data. NFL maximizes the similarity between text features generated from the learnable prompt embeddings and an ensemble of hand-crafted prompts. Extensive experiments on three downstream vision tasks, *i.e.*, image classification, open-vocabulary object

detection, and zero-shot semantic segmentation verify the effectiveness of the proposed approach.

The contributions of this work are summarized as follows:

- We manage to analyze the cause of overfitting problem in CoOp, by measuring the gradient flow in the early and later training stage.
- We propose Subspace Prompt Tuning (*SubPT*) to eliminate the spurious components in gradients during back-propagation, and successfully mitigate overfitting.
- We propose Novel Feature Learner (NFL) to enhance the generalization ability of the learned prompt embedding towards novel categories, needless of image training data.
- Extensive experiments on three downstream vision tasks including image classification, open-vocabulary object detection, and zero-shot semantic segmentation verify the effectiveness of the proposed approach.

II. RELATED WORK

In this section, we briefly revisit the vision-language models and existing prompt tuning methods. Then we review the representative studies on the generalization under data distribution shifts between the training and test set.

A. Vision-Language Models

Conventional multi-modal deep models are usually trained on close-set problems such as object tracking [16]–[21], content generation [22], [23], *etc.* In comparison, vision-language models (VLMs) such as [1], [2], [24], [25] show an impressive ability of understanding infinite open-world visual concepts with the help of language supervision. Being one of the most popular VLMs, CLIP [1] is composed of an image encoder and a text encoder, and is pre-trained on ~ 400 million image-caption pairs to align the image and text to the same feature space in a self-supervised contrastive manner. Towards the downstream vision task such as zero-shot image classification, CLIP can obtain impressive performance with a properly designed prompt template such as “a photo of a [CLASS]”.

B. Prompt Tuning in Vision-Language Models

Many recent works explore the efficient and effective way of adapting VLMs to downstream vision tasks. For example, Zhou *et al.* [9] first report that compared with handcrafted prompt templates, continuous prompt embeddings learned on training samples from the downstream image classification task can contribute to better performances. Based on CoOp [9], prompt tuning methods for complex tasks have also been proposed, such as open-vocabulary object detection [12], [26], zero-shot semantic segmentation [13], continual learning [27], and multi-label image classification [28]. CoCoOp [10] reports that CoOp suffers from overfitting issue and hurts the generalization ability on novel classes and out-of-distribution data. However, CoCoOp still fails to understand the cause of overfitting, and how to deal with the overfitting issue remains an open question. Besides, some other works focus on studying vision prompts, such as tip-adapter [29], colorful prompt tuning [30], visual prompt tuning [31], and neural prompt search [32]. However, since the vision modality is

naturally more complex than the language modality due to the diversity of illumination, view point, domain, *etc.*, vision prompts tend to be less generalizable than text prompts across tasks and datasets. Thus, we only study prompt tuning on the text branch in this paper.

C. Generalization under Data Distribution Shifts

In the machine learning community, the conventional goal is to minimize the total error on the test set, which shares the identical distribution and is independent with the training set. However, such i.i.d assumption is usually not satisfied in the real-world scenario due to the change of environment [33] and occurrence of novel categories [34], and the data distribution shifts refers to the mismatch of distribution between training and test data. How to train reliable and robust models under data distribution shifts has been studied differently in various research areas. As for domain generalization [35]–[37], researchers focus on learning domain-invariant features across training datasets from multiple source domains. As for meta-learning and few-shot learning [38]–[40], researchers have access to a large training set to learn a similarity function, and conduct inference on the query set with the help of a small support set. However, prompt tuning is different from all mentioned works, since only a few training samples from a single domain are provided, and only the prompt embeddings (classifier) rather than visual and text encoders (feature extractor) are trainable.

III. PRELIMINARY

A. Contrastive Language-Image Pre-training (CLIP)

CLIP [1] is composed of two independent encoders, where the visual encoder $f(\cdot)$ maps the input image \mathbf{x} into the feature vector $f(\mathbf{x})$, and the text encoder $g(\cdot)$ maps the input sentence \mathbf{t} into $g(\mathbf{t})$. For clarity, we denote the ℓ_2 -normalized feature as $\mathbf{z} = \frac{f(\mathbf{x})}{\|f(\mathbf{x})\|}$ and $\mathbf{w} = \frac{g(\mathbf{t})}{\|g(\mathbf{t})\|}$ sharing the same dimensionality. The inner product $\mathbf{z}^\top \mathbf{w}$ stands for the semantic similarity between \mathbf{x} and \mathbf{t} .

We revisit the way of utilizing CLIP on zero-shot image classification. In the baseline setting, the prompt is manually designed as “a photo of a [CLASS]”. Given a C -class task, we first prepare C category descriptions by feeding each of category names (already known) into the prompt, and obtain C text features $\{\mathbf{w}_i\}_{i=1}^C$ using the text encoder $g(\cdot)$. Then, given an input image \mathbf{x} , we compute similarity scores between the encoded image feature \mathbf{z} and all text features, and finally get the prediction probability on class y via softmax function as

$$p(y|\mathbf{x}) = \frac{\exp(\mathbf{z}^\top \mathbf{w}_y / \tau)}{\sum_{i=1}^C \exp(\mathbf{z}^\top \mathbf{w}_i / \tau)}. \quad (1)$$

We omit the temperature τ (default as 1.0) in the following sections for simplicity. Since CLIP is pre-trained on millions of noisy image-text pairs, zero-shot CLIP can be directly applied to downstream classification task and achieve satisfying accuracy without any task-related training data (for example, 86.29% on Caltech101 with ResNet-50 [41] visual encoder).

B. Overfitting Issue in CoOp

Formally, Context Optimization (CoOp) [9] first initializes a total of M learnable word embeddings $\mathbf{v} = [\mathbf{v}_1, \dots, \mathbf{v}_M] \in \mathbb{R}^{d \times M}$, then $\mathbf{t}_i = [\mathbf{v}, \mathbf{c}_i]$ concatenates the learnable prompt \mathbf{v} and the fixed category name embedding \mathbf{c}_i is fed to the encoder $g(\cdot)$ and mapped to the text feature \mathbf{w}_i . Under the few-shot setting, CoOp learns the embedding \mathbf{v} on the labeled data $\{(\mathbf{x}_j, y_j)\}$ by minimizing the cross entropy loss:

$$L_{ce}(\mathbf{v}) = - \sum_j \log p(y_j|\mathbf{x}_j). \quad (2)$$

As reported in [9], CoOp boost the classification accuracy on the Caltech101 dataset [42] from 86.29% to 87.53% under the 1-shot setting, with visual encoder being ResNet-50. However, as reported in [10]–[13] and our experimental results, two aspects of overfitting problem limit the effectiveness of CoOp on base classes and novel classes. As shown in Fig. 1(a), the test accuracy on base categories first gets better in early training stage (from 1st to 10th epoch), then gets worse in later training stage (from 11th to 50th epoch). Fig. 1(b) shows that the test accuracy on novel categories keeps declining.

Conditional Context Optimization (CoCoOp) [10] is then proposed to overcome the overfitting issue in CoOp using the image-specific prompt. Specifically, the prompt embedding \mathbf{v} is added with a residual vector, which is generated by a learnable encoder fed with the image feature \mathbf{z} . However, CoCoOp cannot effectively eliminate overfitting in CoOp.

C. Gradient Flow

Gradient flow [43]–[46] is a deterministic model of stochastic gradient descent (SGD), defined by the *total gradient* differential equation:

$$\dot{\Phi}_t = \frac{d\Phi}{dt} = -g(\Phi), \quad g(\Phi) = E_{(x,y) \sim Train} \nabla_{\Phi} L(\Phi, x, y), \quad (3)$$

where $\Phi(t)$ denotes the evolution of model parameters, and $g(\Phi)$ is the average gradient over the entire training set. Consider the update $\Delta\Phi = -g(\Phi) \cdot \Delta t$, where Δt represents the sum of learning rate over time, so SGD can be viewed as a discretization of gradient flow.

IV. METHODOLOGY

In this section, we first study the overfitting problem in prompt tuning by observing the gradient flows (Sec. IV-A), then conduct comparative experiments to identify the cause of overfitting phenomenon (Sec. IV-B). Finally, we propose Subspace Prompt Tuning (*SubPT*) to eliminate the overfitting problem (Sec. IV-C), and introduce Novel Feature Learner (*NFL*) to enhance the generalization performance on novel categories (Sec. IV-D).

A. Analyzing Gradient Flow in Prompt Tuning

The no free lunch theorem [14], [15] states that it is impossible to learn without making proper assumptions on the distribution of training set and test set, thus the i.i.d. assumption and empirical risk minimization (ERM) become the most

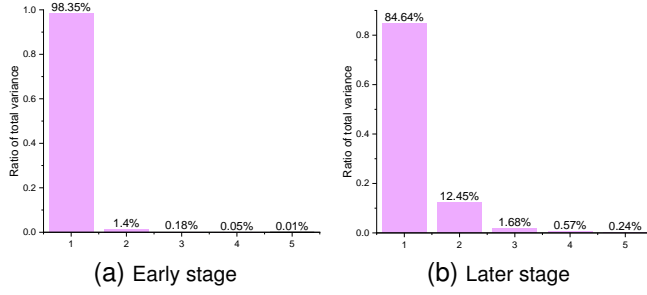


Fig. 2. **The variance distribution of PCA components.** The dataset is Caltech101. We observe that the spectrum of gradient flow is dominated by only a few components. (a) The early training stage (from 1st to 10th epoch). (b) The later training stage (from 31st to 50th epoch).

popular in the machine learning community. However, the i.i.d. assumption does not hold in many practical applications, leading to the learned parameters not generalizable from the training set to the test set. So an intuitive idea to understand the overfitting problem in prompt tuning is that CoOp favors the generalizable/spurious feature direction in the early/later training stage.

To investigate the training direction, we formulate the gradient flow of the learnable prompt \mathbf{v} as

$$\begin{aligned} \dot{\mathbf{v}}_t &= -\nabla L_{ce}(\mathbf{v}_t) \\ &= -\nabla_{\mathbf{v}} g([\mathbf{v}_t, \mathcal{C}])^\top \cdot \nabla_{g([\mathbf{v}_t, \mathcal{C}])} L_{ce}(\mathcal{Z}, g([\mathbf{v}_t, \mathcal{C}])), \end{aligned} \quad (4)$$

where \mathcal{C} and \mathcal{Z} stand for the set of category names and image features appeared in the training process respectively, and L_{ce} refers to the softmax cross entropy loss. The second term can be confirmed as a constant matrix¹ since both \mathcal{C} and \mathcal{Z} are fixed, so the gradient flow $\dot{\mathbf{v}}_t$ is governed by the first term $\nabla_{\mathbf{v}} g([\mathbf{v}_t, \mathcal{C}])$, which denotes the gradient from output to input on the text encoder $g(\cdot)$ and varies over time t . However, it is still laborious to compute $\nabla_{\mathbf{v}} g([\mathbf{v}_t, \mathcal{C}])$. Recalling the recent work [47], Li *et al.* prove that both $\nabla_{\mathbf{v}} g([\mathbf{v}_t, \mathcal{C}])$ and $\dot{\mathbf{v}}_t$ can be approximated by low-rank matrices, since only a small part of eigenvalues dominates the spectrum of neural tangent kernel (NTK) under the infinite-width assumption [48], and NTK is defined as $\Theta_t = \nabla_{\mathbf{v}} g([\mathbf{v}_t, \mathcal{C}]) \cdot \nabla_{\mathbf{v}} g([\mathbf{v}_t, \mathcal{C}])^\top$. In practice, we follow [47] to first conduct an entire process of CoOp training and save the embedding checkpoint when every epoch ends. Then we sample a trajectory of checkpoints $\mathbf{V} = \{\mathbf{v}_{t_1}, \dots, \mathbf{v}_{t_2}\} \in \mathbb{R}^{(t_2-t_1) \times (d \times M)}$ and conduct principal component analysis (PCA) to compute the eigenvectors $\mathbf{U} = \{\mathbf{u}_1, \dots, \mathbf{u}_r\} \in \mathbb{R}^{r \times (d \times M)}$ characterizing the gradient flow $\dot{\mathbf{v}}_t$, since the trajectory can be viewed as a discretization of $\dot{\mathbf{v}}_t$ with some certain affine transformation. The PCA procedure is formulated as

$$\max_{\mathbf{U}} \|\mathbf{V} - \mathbf{V}\mathbf{U}^\top \mathbf{U}\|_F^2, \quad \text{s.t. } \mathbf{U}\mathbf{U}^\top = \mathbf{I}. \quad (5)$$

Note that each checkpoint in \mathbf{V} is centralized, and the eigenvectors in \mathbf{U} are sorted in descending order with respect to eigenvalues. We test with two trajectories within a total of 50 epochs: the early training stage (from 1st to 10th epoch) and

¹It is because that $\nabla_{\mathbf{z}^\top \mathbf{w}} L_{ce} = \mathbf{y} - \sigma(\mathbf{z}^\top \mathbf{w})$ and $\nabla_{\mathbf{w}} \mathbf{z}^\top \mathbf{w} = \mathbf{z}$. (\mathbf{y} denotes the labels in training set, $\sigma(\cdot)$ denote the softmax function, and $\mathbf{z} \in \mathcal{Z}$).

TABLE I
DISPLAY ON THE INNER PRODUCT BETWEEN TWO DOMINANT EIGENVECTORS ACROSS VARIOUS DATASETS.

Dataset	Caltech101	Oxford Pets	Stanford Cars	DTD
Inner product	-0.0099	-0.0124	-0.0547	-0.0559

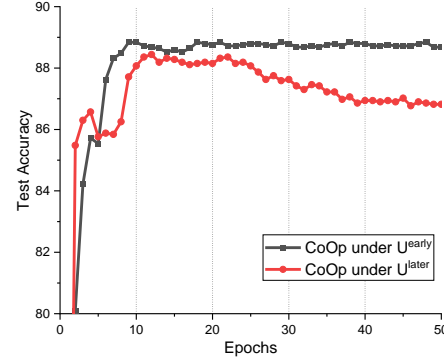


Fig. 3. Comparison on the base class test set accuracy during the training process with \mathbf{U} being $\mathbf{U}^{\text{early}}$ and $\mathbf{U}^{\text{later}}$, respectively. The dataset is Caltech101. We observe that the overfitting phenomenon occurs with \mathbf{U} being $\mathbf{U}^{\text{later}}$, and can be mitigated using $\mathbf{U}^{\text{early}}$.

the later training stage (from 31st to 50th epoch). As displayed in Fig. 2, the first eigenvector always occupies about 90% of total variance, agreeing with the above analysis. As a result, we can characterize the gradient flow of each training stage $\dot{\mathbf{v}}_t$ with its first eigenvector \mathbf{u}_1 .

Back to our initial idea, we now measure the inner product between the first eigenvectors of gradient flows in the early and later training stage across different datasets. As shown in Table. I, the inner product is always close to zero, meaning that the two gradient flows are almost orthogonal. Such experimental results reveal that CoOp does learn different features in early and later training stages.

B. Cause of Overfitting

Now we design experiments to investigate whether CoOp favors generalizable/spurious feature in the early/later training stage, leading to the non-overfitting/overfitting phenomenon. For clarity, we first provide the experiment details, then give the explanation. Specifically, we first conduct an entire process of CoOp training and save the embedding checkpoint at the end of each epoch. Based on the observations in Sec. IV-A, we compute two sets of eigenvectors ($\mathbf{U}^{\text{early}}$ and $\mathbf{U}^{\text{later}}$) from the checkpoints sampled in early and later training stages ($\{\mathbf{v}_t\}_{t=1}^{10}$ and $\{\mathbf{v}_t\}_{t=31}^{50}$) to represent the corresponding gradient flows, respectively. Then, we re-run CoOp twice from the same initial embedding, and force two training processes towards the main components of these two gradient flows, respectively. Similar with [47] and [49], we multiply the gradient in each training step by the projection matrix $\mathbf{U}^\top \mathbf{U} \in \mathbb{R}^{(d \times M) \times (d \times M)}$, and the update formula of CoOp can be re-written as

$$\mathbf{v} \leftarrow \mathbf{v} - \alpha \cdot \mathbf{U}^\top \mathbf{U} \frac{\partial L_{ce}(\mathbf{v})}{\partial \mathbf{v}}. \quad (6)$$

Note that we slightly abuse the notations here as both \mathbf{v} and $\partial L_{ce}(\mathbf{v})/\partial \mathbf{v}$ are vectorized. We omit the superscript of \mathbf{U}

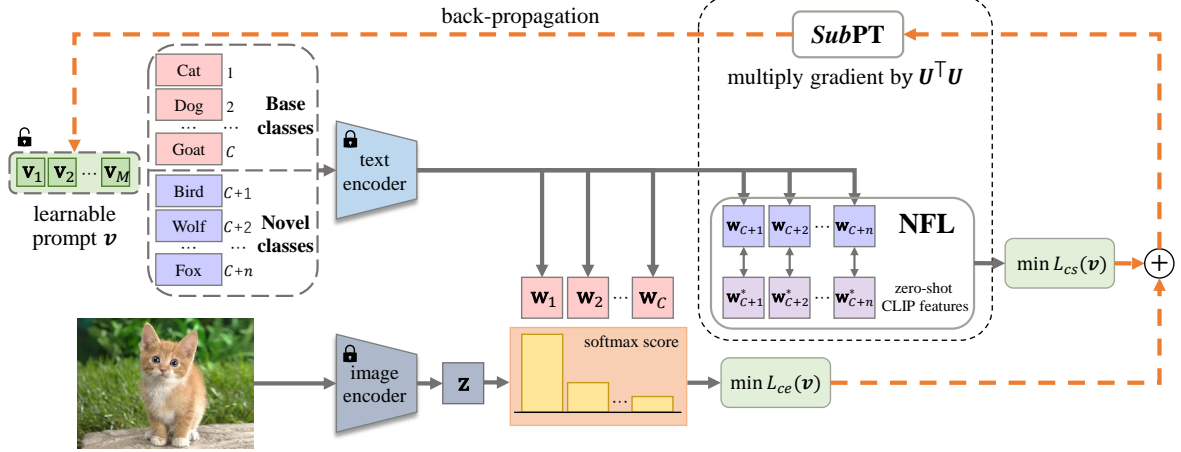


Fig. 4. **Overview of the proposed Subspace Prompt Tuning (SubPT) and Novel Feature Learner (NFL)**, surrounded by the black dotted box. To eliminate spurious components and mitigate overfitting, we project the gradient onto the low-rank **subspace** spanned by the dominant eigenvectors \mathbf{U} of early-stage gradient flow during back-propagation. **NFL** learns text features towards zero-shot CLIP features on novel categories to enhance the generalization ability of the learned prompt embedding beyond the training set.

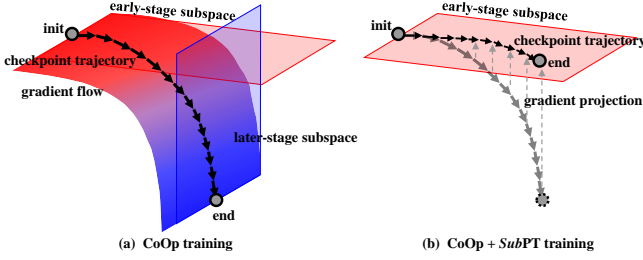


Fig. 5. An intuitive understanding on **Subspace Prompt Tuning (SubPT)**. We first construct the subspace spanned by prompt embedding checkpoints in early training stage, then we re-run CoOp from the same initial point and project gradients onto the constructed subspace in back-propagation to eliminate the spurious components. The rationale behind **SubPT** lies that the spurious components are orthogonal to the early-stage subspace.

without loss of generality. α denotes the learning rate. In fact, the gradient vector $\partial L_{ce}(\mathbf{v}) / \partial \mathbf{v}$ is projected onto the low-rank subspace spanned by eigenvectors, so the components in the directions orthogonal to eigenvectors \mathbf{U} are eliminated. Thus, when we specify \mathbf{U} in Eq. (6) as $\mathbf{U}^{\text{early}}$ or $\mathbf{U}^{\text{later}}$, the entire training process is forced towards the corresponding direction.

We take the Caltech101 [42] dataset under 1-shot setting for example. As shown in Fig. 3, with \mathbf{U} being $\mathbf{U}^{\text{early}}$, the test set performance increases to the best and never drops during the whole training process. In contrast, with \mathbf{U} being $\mathbf{U}^{\text{later}}$, the test set performance shares the similar trend with that of the original CoOp. Such experimental results indicates that CoOp does favor spurious features in the later training stage, leading to the overfitting phenomenon.

Remark. We emphasize the fact about the above experiment that when specifying \mathbf{U} as $\mathbf{U}^{\text{later}}$, the test performance first gets better than gets worse, instead of keeping decreasing as the original CoOp does from 31st to 50th epoch. It is because that the PCA procedure (refer to Eq. (5)) takes an unordered set of embedding checkpoints as inputs, so the computed eigenvectors $\mathbf{U}^{\text{later}}$ reflect the learned feature direction, instead of the trajectory direction.

C. Subspace Prompt Tuning (SubPT)

Given the above observations and analysis, now it is easy and straightforward to mitigate the overfitting issue in prompt tuning in three steps.

- Step 1: Conduct prompt tuning and save the embedding checkpoint \mathbf{v}_t at the end of every epoch.
- Step 2: Compute dominate eigenvectors $\mathbf{U}^{\text{early}} = \{\mathbf{u}_1, \dots, \mathbf{u}_r\}$ of the saved checkpoints $\mathbf{V}_{\text{early}} = \{\mathbf{v}_1, \dots, \mathbf{v}_{t_{\text{early}}}\}$ in the specified early training stage (refer to Eq. (5)). t_{early} denotes the last epoch of the early training stage. r represents the number of eigenvectors ($r \leq t_{\text{early}}$).
- Step 3: Re-run prompt tuning from the same initial point, and project the gradients in back-propagation onto the low-rank subspace spanned by $\mathbf{U}^{\text{early}}$ during the entire training process (refer to Eq. (6)).

We name this approach Subspace Prompt Tuning (**SubPT**), where the generalizable components in gradients are maintained and the spurious components are eliminated during the multiplication process (see Figs. 4 and 5 for the overview of proposed method and the intuitive understanding). Figs. 1(a) and 1(b) demonstrate that **SubPT** can address the overfitting issue effectively.

D. Novel Feature Learner (NFL)

This section presents Novel Feature Learner (NFL) to enhance the generalization ability of the learned prompt towards novel classes beyond the training set without any image training data. As shown in Fig. 4, NFL contains text features on novel categories generated from learnable prompts, zero-shot CLIP features in correspondence, and a feature similarity loss L_{cs} . We first encode the learnable prompt embedding combining novel category name embeddings into text features $\{\mathbf{w}_i\}_{i=C+1}^{C+n}$ with the text encoder $g(\cdot)$. Then, we utilize zero-shot CLIP to obtain corresponding text features $\{\mathbf{w}_i^*\}_{i=C+1}^{C+n}$ with the handcrafted prompts, and further optimize the feature similarities between them with L_{cs} . We give more details in the following part.

Novel category selection. We consider two following scenes. If the novel category names are unknown during training (such as the few-shot classification), we randomly select n categories from 1000 ImageNet [50] categories, disjoint from the base categories within the training set. In experiments, we observe that the performance gain brought by NFL remains similar as n increases from 100 to 1000, so we fix n as 100 for computational convenience. Besides, if the novel category names are known during training (such as the base-to-novel classification), then we directly utilize these novel category names for NFL.

Zero-shot CLIP features. To obtain corresponding zero-shot CLIP features, we select 80 handcrafted prompt templates provided by [1] such as “a good photo of the [CLASS]” and “an origami [CLASS]”, and further compute the averaged text feature for each category.

Feature similarity loss. Since the zero-shot CLIP has great generalization capability, we propose to minimize the feature similarities between $\{\mathbf{w}_i\}_{i=C+1}^{C+n}$ and $\{\mathbf{w}_i^*\}_{i=C+1}^{C+n}$ to enhance the performance of learned prompt embeddings towards novel categories. We choose the cosine similarity as loss function, and the NFL is formulated as

$$L_{cs}(\mathbf{v}) = \frac{1}{n} \sum_{i=C+1}^{C+n} (1 - \mathbf{w}_i^\top \mathbf{w}_i^*). \quad (7)$$

Note that NFL does not involve any image training data, so it is convenient to apply as an extra loss term during training, and the total loss is written as

$$L(\mathbf{v}) = L_{ce}(\mathbf{v}) + \lambda \cdot L_{cs}(\mathbf{v}). \quad (8)$$

V. EXPERIMENTS

In this section, we evaluate our proposed *SubPT* and NFL on three downstream vision tasks including image classification, open-vocabulary object detection, and zero-shot semantic segmentation. We describe the datasets and evaluation metrics in detail, along with baselines and implementation details. We also conduct ablation studies on all the hyper-parameters in the proposed approach.

A. Image Classification

We consider three problem settings for the image classification task, that are *few-shot classification*, *base-to-novel generalization*, and *domain generalization*.

Datasets. For few-shot classification and base-to-novel generalization, we follow CoOp [9] and CoCoOp [10] to rely on 11 classification datasets. These include generic object classification datasets (*i.e.* ImageNet [50] and Caltech101 [42]), fine-grained visual classification (*i.e.* Oxford Pets [51], Stanford Cars [52], Flowers 102 [53], Food 101 [54] and FGVC Aircraft [55]), scene recognition (*i.e.* SUN 397 [56]), texture classification (*i.e.* DTD [57]), satellite imagery recognition (*i.e.* EuroSAT [58]), and action recognition (*i.e.* UCF 101 [59]). For base-to-novel generalization, we split the first half of categories as base classes and the second half as novel classes within each dataset. For domain generalization, we choose

ImageNet as source domain dataset and evaluate performance on four target domain datasets: ImageNet-V2 [60], ImageNet-Sketch [61], ImageNet-A [62], and ImageNet-R [63].

Evaluation Metrics. For all problem settings, we report the average accuracy over three different random seeds. We also report the harmonic mean $HM = 2 \times (\text{base} \times \text{new}) / (\text{base} + \text{new})$ for base-to-novel generalization.

Baselines. We compare our proposed approach with both zero-shot CLIP [1] (based on the handcrafted prompt) and CoOp [9]. Since CoCoOp [10] can degrade the base accuracy of CoOp as reported in [10] and is only designed to improve the generalization ability of learned prompt, we only compare with CoCoOp on the base-to-novel generalization and domain generalization settings.

Implementation Details. We follow the official implementation of CoOp² [9] and CoCoOp³ [10] to adopt few-shot learning for all problem settings. For few-shot classification, we conduct prompt tuning with 1, 2, 4, 8, and 16 shots respectively and evaluate performance on the entire test set. For base-to-novel generalization and domain generalization, we adopt the 4-shots training. The prompt length M is fixed as 16 and the prompt embedding is initialized with Gaussian distribution $\mathcal{N}(0, 0.02)$. We follow the same training schedule and data augmentation strategies in CoOp [9]. The visual encoder is specified as ResNet-50 for all experiments.

There are only two hyper-parameters in *SubPT*, that are t_{early} and r , and we will study the dependency on them in the ablations later. We set (t_{early}, r) as (10, 5) for 1 shot, (20, 10) for 2 shots, (30, 10) for 4 shots, (40, 10) for 8 shots, and (50, 10) for 16 shots. We observe in experiments that the overfitting problem does not occur on the Flowers 102 and EuroSAT datasets, so we set t_{early} as t_{total} for these two datasets specifically. For NFL, we set the loss weight λ as 1.0.

Few-Shot Classification Results. Fig. 6 shows the comparison with baseline approaches on 11 classification datasets. The average accuracies over all datasets are also displayed in the first subfigure. In comparison with the zero-shot CLIP baseline, the proposed *SubPT* can consistently and substantially outperform the average accuracy by 2.37% with 1 training sample per class and 15.45% with 16 training samples per class. Then NFL can further push the accuracy higher by 0.11% ~ 0.73%. Besides, *SubPT* plus NFL can also boost the average performance of CoOp with 3.14% relative gain in 1-shot and with 1.23% relative gain in 16-shot. For example on Food 101 dataset, the performance of CoOp+*SubPT*+NFL can surpass that of CoOp by 3.57% relatively in 1-shot and 3.84% relatively in 16-shot. These results validate the effectiveness of both *SubPT* and NFL on mitigating the overfitting issue in CoOp.

Base-to-Novel Generalization Results. Table II presents the performance of *SubPT* and NFL in the base-to-novel generalization setting on 11 classification datasets.

As can be seen, the overfitting problem in CoOp is reflected by the divergence of test set accuracies between base and novel classes. For example, CoOp can boost the average per-

²<https://github.com/KaiyangZhou/CoOp/blob/main/COOP.md>

³<https://github.com/KaiyangZhou/CoOp/blob/main/COCOOP.md>

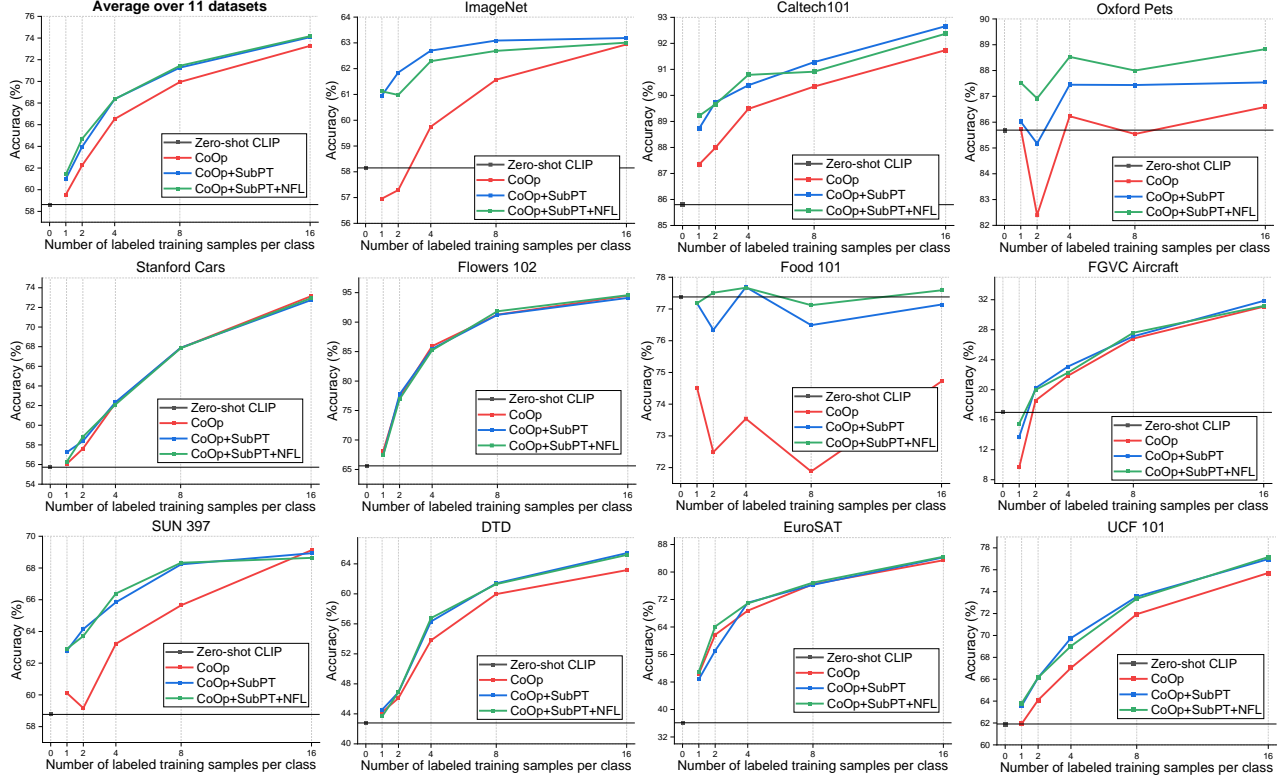


Fig. 6. Comparison with zero-shot CLIP and CoOp on few-shot classification above 11 datasets. Our proposed approaches “CoOp+SubPT” and “CoOp+SubPT+NFL” can consistently improve the performances of CoOp.

formance of zero-shot CLIP on base classes with an absolute 6.93% margin over 11 datasets, but can also degrade CLIP’s performance on novel classes by an absolute 10.30% margin. CoCoOp can remedy the CoOp’s novel class accuracy with 1.67% by changing the static prompts into dynamic ones, but the remedied accuracy is still far below that of zero-shot CLIP (60.42% vs 69.05%). In contrast, adding *SubPT* to CoOp mitigates the overfitting problem on both base and novel classes, as the base accuracy improves from 72.10% to 72.57% and novel accuracy improves from 58.75% to 62.30%. Besides, NFL can further raise the novel accuracy up to 68.17% and 69.32% respectively, illustrating the effectiveness of NFL. In detail, Fig. 7 depicts the absolute performance improvement of *SubPT* and NFL over CoOp and CoCoOp in terms of the harmonic mean accuracy. We observe that our proposed approach can consistently improve CoOp over 11 datasets and also surpass CoCoOp except the EuroSAT dataset.

Domain Generalization Results. As we discuss in Sec. IV-A, CoOp learns both generalizable and spurious features during the entire training process, while the latter can degrade the generalization ability of learned prompt embeddings onto the out-of-distribution and adversarial datasets. As displayed in Table III, CoOp’s test set accuracy on four target domain datasets are always below that of the original ImageNet, though all of these datasets share the same categories. Similar with the base-to-novel generalization setting, CoCoOp can still enhance the generalization ability of CoOp but with insignificant improvements. In comparison, adding *SubPT* to CoOp can persistently increase the performance of CoOp

and even outperform that of zero-shot CLIP over four target datasets (for example, 57.58% vs 56.00% on ImageNet-R), which verifies that our proposed *SubPT* can eliminate the spurious features during training. We note that adding NFL to CoOp plus *SubPT* can slightly harm the performance. The reason lies that the novel category names adopted in NFL are all collected from ImageNet, so NFL drags the corresponding performance back to that of the zero-shot CLIP.

B. Open-Vocabulary Object Detection

Now we consider more challenging downstream vision task, that is *open-vocabulary object detection (OVOD)*.

Datasets and Evaluation Metrics. We follow the state-of-the-art work PromptDet [12] to conduct experiments on the LVIS dataset [64], which is annotated with bounding boxes and divided into 866 base categories and 337 novel categories. For evaluation on LVIS v1.0 minival set, we report the mask Average Precision for novel categories AP_{novel} , where a higher score indicates a better generalization onto novel category objects beyond the training set.

Baselines. In terms of the prompts utilized in OVOD, we select both the zero-shot CLIP baseline with manual prompt “a photo of [CLASS]” and the Regional Prompt Learning (RPL) [12] as baselines, where RPL learns continuous prompt embedding on the cropped object patches within base categories in the CoOp manner. To examine the ability of *SubPT* against over-fitting problem, we equip RPL with *SubPT* to learn better prompt embeddings for OVOD.

TABLE II

COMPARISON WITH STATE-OF-THE-ART APPROACHES ON BASE-TO-NOVEL GENERALIZATION. HM STANDS FOR HARMONIC MEAN. **BEST** AND **SECOND BEST** RESULTS ARE HIGHLIGHTED.

	Average			ImageNet			Caltech101		
	Base	Novel	HM	Base	Novel	HM	Base	Novel	HM
Zero-shot CLIP	65.17	69.05	66.94	64.39	60.05	62.14	90.77	91.05	90.91
CoOp	72.10	58.75	63.90	64.25	54.99	59.26	94.00	87.37	90.56
CoCoOp	71.91	60.42	65.19	66.49	58.54	62.26	94.36	86.10	90.04
CoOp + SubPT	72.57	62.30	66.37	66.91	60.32	63.44	94.35	89.27	91.74
CoOp + SubPT + NFL	72.96	66.91	69.32	66.14	61.16	63.55	94.77	92.10	93.42
	Oxford Pets			Stanford Cars			Flowers 102		
	Base	Novel	HM	Base	Novel	HM	Base	Novel	HM
Zero-shot CLIP	90.06	94.18	92.07	55.32	66.65	60.46	69.14	73.97	71.47
CoOp	89.67	92.34	90.99	62.57	55.24	58.68	86.80	63.55	73.38
CoCoOp	87.75	90.16	88.94	61.32	56.97	59.07	87.08	62.62	72.85
CoOp + SubPT	90.96	92.60	91.77	62.67	58.83	60.69	88.75	63.22	73.84
CoOp + SubPT + NFL	91.65	95.32	93.45	61.08	65.82	63.36	88.19	71.68	79.08
	Food 101			FGVC Aircraft			SUN 397		
	Base	Novel	HM	Base	Novel	HM	Base	Novel	HM
Zero-shot CLIP	83.59	85.01	84.29	18.79	25.97	21.80	66.78	70.51	68.59
CoOp	78.59	77.86	78.22	22.63	16.92	19.36	71.16	62.20	66.38
CoCoOp	78.53	78.31	78.42	21.67	16.68	18.85	70.18	64.29	67.11
CoOp + SubPT	80.76	80.85	80.80	19.09	21.78	20.35	72.37	68.14	70.19
CoOp + SubPT + NFL	82.20	84.14	83.16	22.99	25.13	24.01	73.35	71.44	72.38
	DTD			EuroSAT			UCF 101		
	Base	Novel	HM	Base	Novel	HM	Base	Novel	HM
Zero-shot CLIP	54.17	56.16	55.15	54.83	66.18	59.97	69.03	69.82	69.42
CoOp	66.09	42.75	51.92	85.10	35.67	50.27	72.23	57.33	63.92
CoCoOp	65.74	41.55	50.92	85.74	51.97	64.71	72.13	57.44	63.95
CoOp + SubPT	66.28	46.50	54.66	81.98	40.79	54.48	74.10	63.01	68.11
CoOp + SubPT + NFL	63.73	52.33	57.47	85.71	49.26	62.56	72.71	67.59	70.06

Implementation Details. Similar with the RPL process in PromptDet [12], we choose ViT-B/32 as the visual encoder backbone and conduct 1-shot training. After RPL, we conduct object detector training over the Mask-RCNN [65] architecture with a ResNet-50-FPN backbone and train 12 epochs for all baselines, based on the official implementation of PromptDet⁴. Note that we omit the self-training procedure in PromptDet [12] for fair comparisons.

Open-Vocabulary Object Detection Results. As reported in Table IV, RPL in 1-shot setting can decrease the AP_{novel} score from 7.4% to 6.4% compared with the zero-shot baseline, indicating the ineffectiveness of RPL under low-shots condition, while our proposed SubPT can boost RPL’s detection performance up to 9.7%, surpassing the zero-shot baseline.

C. Zero-Shot Semantic Segmentation

Lastly, we consider the challenging downstream vision task, that is *zero-shot semantic segmentation*.

Datasets and Evaluation Metrics. We follow the recent work ZSSEG [13] and rely on the COCO stuff [66] dataset containing 171 annotated categories, further divided into 156 base categories and 15 novel categories. We consider four evaluation metrics on 5k validation images, *i.e.*, mean intersection over union across all classes (mIoU) and only novel

categories (mIoU-novel), mean pixel accuracy averaged across classes (mACC), and pixel-wise classification accuracy on novel categories (pACC-novel).

Baselines and Implementation Details. To conduct zero-shot semantic segmentation, we follow the pipeline proposed in ZSSEG⁵ [13] containing two procedures, that are mask proposal generation and region classification via CLIP. For the latter procedure, we implement our proposed SubPT into conventional prompt learning to verify the effectiveness, with 2 training samples per class. The ViT-B/16 visual encoder is utilized in CLIP, and the MaskFormer [67] model with ResNet-50 is selected as backbone for semantic segmentation.

Zero-Shot Semantic Segmentation Results. Table V illustrates that learnable prompts can improve the classification accuracy on image pixels within novel categories (mIoU-novel and pACC-novel) than manual prompts, while our SubPT can further enhance the performances with large margins, 32.84% vs 29.61% on mIoU-novel for example. These results verify the effectiveness of SubPT across various downstream tasks.

D. Ablative Study

In this section, we ablate all the hyper-parameters in the proposed SubPT. Also, we compare the training time among CoOp, CoCoOp, and our proposed method.

⁴<https://github.com/fcjian/PromptDet>

⁵https://github.com/MendelXu/zsseg_baseline

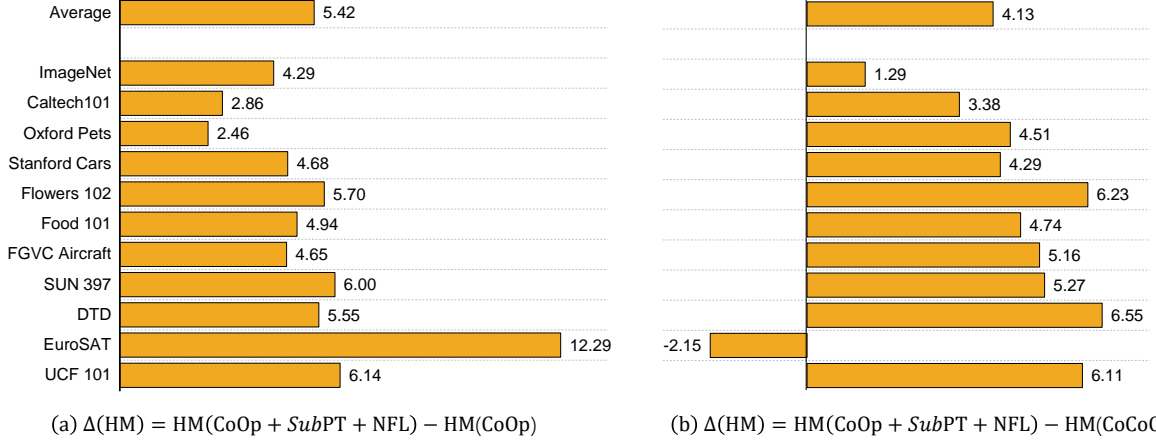


Fig. 7. **Absolute performance improvement of the proposed approach over CoOp and CoCoOp** in terms of harmonic mean accuracy over 11 classification datasets. SubPT and NFL can always enhance the performance of CoOp and surpass that of CoCoOp in 10 out of 11 datasets.

TABLE III
COMPARISON WITH STATE-OF-THE-ART APPROACHES ON DOMAIN GENERALIZATION. **BEST** AND **SECOND BEST** RESULTS ARE HIGHLIGHTED.

	Source	Target			
		ImageNet	ImageNet-V2	ImageNet-Sketch	ImageNet-A
Zero-shot CLIP	58.18	51.34	33.32	21.65	56.00
CoOp	59.74	52.52	31.42	22.25	53.51
CoCoOp	61.01	53.87	32.65	22.56	54.31
CoOp + SubPT	62.48	55.36	34.73	23.95	57.58
CoOp + SubPT + NFL	61.53	54.21	33.32	23.19	57.24

TABLE IV
PERFORMANCE ON OPEN-VOCABULARY OBJECT DETECTION. **BEST** RESULTS ARE HIGHLIGHTED.

Model	RPL	SubPT	shots	AP _{novel}
Baseline (manual prompt)			0	7.4
PromptDet_R_50_FPN_1x	✓		1	6.4
PromptDet_R_50_FPN_1x	✓	✓	1	9.7 (+3.3)

TABLE V
PERFORMANCE ON ZERO-SHOT SEMANTIC SEGMENTATION. **BEST** RESULTS ARE HIGHLIGHTED.

Text prompt	mIoU	mACC	mIoU-novel	pACC-novel
Manual	36.99	50.97	27.29	29.48
Learnt	35.88	50.68	29.61	39.83
Learnt + SubPT	37.89	51.36	32.84	42.13

Effect of t_{early} in SubPT. There exist only two hyperparameters (t_{early} , r) in SubPT, where t_{early} denotes the last epoch of the early training stage. As presented in Sec. IV-B, we propose to eliminate the overfitting problem by multiplying the gradient by eigenvectors representing the early-stage gradient flow during back-propagation. Since t_{early} defines the range of early training stage, it can decide the quality of computed U^{early} and further influence the effect of SubPT. As depicted in Table VI, a larger t_{early} leads to less satisfying accuracies, where $t_{\text{early}} = 0$ indicates the original CoOp for comparison. Besides, the performance approximate to that of original CoOp when t_{early} equals the epoch number, indicating that the computed eigenvectors U^{early} represents the gradient flow

TABLE VI
ABLATION STUDY ON t_{early} IN SubPT. **BEST** RESULTS ARE HIGHLIGHTED.

Dataset	shots	epoch	t_{early}					
			0	10	20	30	40	50
Caltech101	1	50	87.37	88.72	88.76	88.80	88.48	88.19
			87.99	89.52	88.46	88.15	88.03	87.79
	2	100	0	20	40	60	80	100
			89.48	90.39	90.10	89.17	89.21	89.49
	4	100	0	30	40	60	80	100
			74.52	77.18	75.83	75.52	75.02	74.45
Food 101	1	50	0	10	20	30	40	50
			72.48	76.34	73.69	72.93	72.58	72.28
	2	100	0	20	40	60	80	100
			73.54	77.69	77.41	76.32	75.97	75.71
	4	100	0	30	40	60	80	100
			73.54	77.69	77.41	76.32	75.97	75.71

of the entire training process.

Effect of the subspace rank r in SubPT. We investigate how the subspace rank r , which is the number of eigenvectors in U^{early} , can affect the performance of SubPT. As can be seen in Table VII, the performance of CoOp+SubPT is robust across different values of subspace rank r . This can be explained by the fact that the spectrum of gradient flow is dominated by only a few components as presented in Sec. IV-A.

Effect of number of novel category names in NFL. Table VIII shows the effect of the number of novel category names in NFL. Increasing the number from 100 to 500 will not bring obvious performance improvements, so we fix the number n as 100 by default if not specified.

TABLE VII
ABLATION STUDY ON THE SUBSPACE RANK r IN *SubPT*. **BEST** RESULTS ARE HIGHLIGHTED.

CoOp + <i>SubPT</i>	subspace rank r					
	5	10	15	20	25	30
Caltech101	90.22	90.39	90.26	90.39	90.55	90.51
Food 101	77.62	77.69	77.93	78.04	78.02	78.00

TABLE VIII
ABLATION STUDY ON THE NUMBER OF NOVEL CATEGORY NAMES IN NFL.

CoOp + NFL	number of novel category names in NFL				
	1	10	100	200	500
Caltech101	88.32	88.82	88.80	88.56	88.69
Food101	74.91	75.85	76.02	75.99	76.09

Computational efficiency. We compare the average time cost in a single iteration under 1-shot setting over the Caltech101 dataset, trained on an Nvidia RTX A6000 GPU. We observe from Table IX that both *SubPT* and NFL will not burden the efficiency of CoOp, and are much more effective than CoCoOp (0.22s vs 1.40s).

Quantitative analysis on gradient norm. As *SubPT* eliminates the spurious components in gradients during back-propagation, it is reasonable that the gradient norm in the later training stage is smaller than that of early stage. We record the gradient norms during the entire training process, and observe corresponding results as shown in Fig. 8.

VI. CONCLUSION

In this paper, we first revisit two aspects of overfitting problem appeared in the well-known prompt tuning approach CoOp. Then we explore the cause of overfitting by measuring the gradient flow, and observe in experiments that CoOp learns different orthogonal features at the early and later training stage, which leads to the non-overfitting and overfitting phenomenon, respectively. Based on our observation and discussion, we then propose Subspace Prompt Tuning (*SubPT*). During the whole training process, *SubPT* projects the gradients in back-propagation onto the low-rank subspace spanned by the eigenvectors representing the early-stage gradient flow, and successfully mitigate the overfitting problem. Besides, we equip CoOp with the specially designed Novel Feature Learner (NFL) to improve the generalization ability of the learned prompt towards the novel classes out of the training set, needless of image training data. Extensive experiments on image classification, open-vocabulary object detection, and zero-shot semantic segmentation verify the effectiveness of the proposed method. Our future work will include designing more robust and general subspace for multi-modal prompt tuning.

REFERENCES

[1] A. Radford, J. W. Kim, C. Hallacy, A. Ramesh, G. Goh, S. Agarwal, G. Sastry, A. Askell, P. Mishkin, J. Clark *et al.*, “Learning transferable visual models from natural language supervision,” in *International Conference on Machine Learning*. PMLR, 2021, pp. 8748–8763.

TABLE IX
COMPARISON ON AVERAGE TIME COST IN A SINGLE ITERATION UNDER 1-SHOT SETTING.

Method	<i>SubPT</i>	NFL	Training time (s)
CoOp			0.19
CoOp	✓		0.20
CoOp		✓	0.20
CoOp	✓	✓	0.22
CoCoOp			1.40

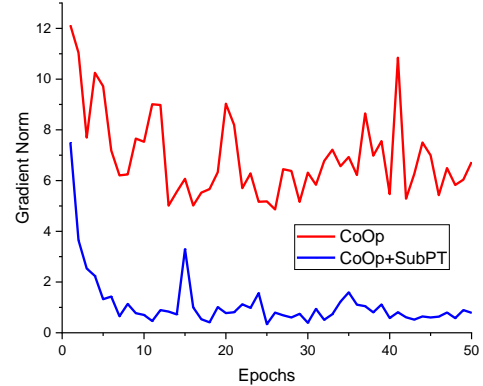


Fig. 8. Comparison on gradient norm between CoOp and CoOp+SubPT during the entire training process.

[2] C. Jia, Y. Yang, Y. Xia, Y.-T. Chen, Z. Parekh, H. Pham, Q. Le, Y.-H. Sung, Z. Li, and T. Duerig, “Scaling up visual and vision-language representation learning with noisy text supervision,” in *International Conference on Machine Learning*. PMLR, 2021, pp. 4904–4916.

[3] R. Bommasani, D. A. Hudson, E. Adeli, R. Altman, S. Arora, S. von Arx, M. S. Bernstein, J. Bohg, A. Bosselut, E. Brunskill *et al.*, “On the opportunities and risks of foundation models,” *arXiv preprint arXiv:2108.07258*, 2021.

[4] T. Mei, J. J. Corso, G. Kim, J. Luo, C. Shen, and H. Zhang, “Guest editorial introduction to the special section on video and language,” *IEEE Transactions on Circuits and Systems for Video Technology*, vol. 32, no. 1, pp. 1–4, 2022.

[5] H. Li, L. Fang, and T. Zhang, “Guest editorial introduction to the special section on intelligent visual content analysis and understanding,” *IEEE Transactions on Circuits and Systems for Video Technology*, vol. 30, no. 12, pp. 4405–4408, 2020.

[6] W. Zhang, C. Ma, Q. Wu, and X. Yang, “Language-guided navigation via cross-modal grounding and alternate adversarial learning,” *IEEE Transactions on Circuits and Systems for Video Technology*, vol. 31, no. 9, pp. 3469–3481, 2020.

[7] B. Lester, R. Al-Rfou, and N. Constant, “The power of scale for parameter-efficient prompt tuning,” in *Proceedings of the 2021 Conference on Empirical Methods in Natural Language Processing*, 2021, pp. 3045–3059.

[8] X. L. Li and P. Liang, “Prefix-tuning: Optimizing continuous prompts for generation,” in *Proceedings of the 59th Annual Meeting of the Association for Computational Linguistics and the 11th International Joint Conference on Natural Language Processing (Volume 1: Long Papers)*, 2021, pp. 4582–4597.

[9] K. Zhou, J. Yang, C. C. Loy, and Z. Liu, “Learning to prompt for vision-language models,” *International Journal of Computer Vision*, vol. 130, no. 9, pp. 2337–2348, 2022.

[10] K. Zhou, J. Yang, C. C. Loy, and Z. Liu, “Conditional prompt learning for vision-language models,” in *Proceedings of the IEEE/CVF Conference on Computer Vision and Pattern Recognition*, 2022, pp. 16 816–16 825.

[11] B. Zhu, Y. Niu, Y. Han, Y. Wu, and H. Zhang, “Prompt-aligned gradient for prompt tuning,” *arXiv preprint arXiv:2205.14865*, 2022.

[12] C. Feng, Y. Zhong, Z. Jie, X. Chu, H. Ren, X. Wei, W. Xie, and L. Ma, “Promptdet: Towards open-vocabulary detection using uncurated

images,” in *European Conference on Computer Vision*. Springer, 2022, pp. 701–717.

[13] M. Xu, Z. Zhang, F. Wei, Y. Lin, Y. Cao, H. Hu, and X. Bai, “A simple baseline for open-vocabulary semantic segmentation with pre-trained vision-language model,” in *European Conference on Computer Vision*. Springer, 2022, pp. 736–753.

[14] D. H. Wolpert, “The lack of a priori distinctions between learning algorithms,” *Neural computation*, vol. 8, no. 7, pp. 1341–1390, 1996.

[15] M. Pezeshki, O. Kaba, Y. Bengio, A. C. Courville, D. Precup, and G. Lajoie, “Gradient starvation: A learning proclivity in neural networks,” *Advances in Neural Information Processing Systems*, vol. 34, pp. 1256–1272, 2021.

[16] W. Zhang, H. Zhou, S. Sun, Z. Wang, J. Shi, and C. C. Loy, “Robust multi-modality multi-object tracking,” in *Proceedings of the IEEE/CVF International Conference on Computer Vision*, 2019, pp. 2365–2374.

[17] H. Zhang, L. Cheng, T. Zhang, Y. Wang, W. Zhang, and J. Zhang, “Target-distractor aware deep tracking with discriminative enhancement learning loss,” *IEEE Transactions on Circuits and Systems for Video Technology*, 2022.

[18] Z. Zhou, X. Li, T. Zhang, H. Wang, and Z. He, “Object tracking via spatial-temporal memory network,” *IEEE Transactions on Circuits and Systems for Video Technology*, vol. 32, no. 5, pp. 2976–2989, 2021.

[19] J. Wei, Y. Wang, Y. Li, R. He, and Z. Sun, “Cross-spectral iris recognition by learning device-specific band,” *IEEE Transactions on Circuits and Systems for Video Technology*, 2021.

[20] Q. Li, X. Zhao, R. He, and K. Huang, “Recurrent prediction with spatio-temporal attention for crowd attribute recognition,” *IEEE Transactions on Circuits and Systems for Video Technology*, vol. 30, no. 7, pp. 2167–2177, 2019.

[21] W. Wang, C. Wang, S. Liu, T. Zhang, and X. Cao, “Robust target tracking by online random forests and superpixels,” *IEEE Transactions on Circuits and Systems for Video Technology*, vol. 28, no. 7, pp. 1609–1622, 2017.

[22] L. Song, W. Wu, C. Fu, C. C. Loy, and R. He, “Audio-driven dubbing for user generated contents via style-aware semi-parametric synthesis,” *IEEE Transactions on Circuits and Systems for Video Technology*, 2022.

[23] L. Yu, J. Yu, M. Li, and Q. Ling, “Multimodal inputs driven talking face generation with spatial-temporal dependency,” *IEEE Transactions on Circuits and Systems for Video Technology*, vol. 31, no. 1, pp. 203–216, 2020.

[24] X. Zhai, X. Wang, B. Mustafa, A. Steiner, D. Keysers, A. Kolesnikov, and L. Beyer, “Lit: Zero-shot transfer with locked-image text tuning,” in *Proceedings of the IEEE/CVF Conference on Computer Vision and Pattern Recognition*, 2022, pp. 18123–18133.

[25] J.-B. Alayrac, J. Donahue, P. Luc, A. Miech, I. Barr, Y. Hasson, K. Lenc, A. Mensch, K. Millican, M. Reynolds *et al.*, “Flamingo: a visual language model for few-shot learning,” *arXiv preprint arXiv:2204.14198*, 2022.

[26] Y. Du, F. Wei, Z. Zhang, M. Shi, Y. Gao, and G. Li, “Learning to prompt for open-vocabulary object detection with vision-language model,” in *Proceedings of the IEEE/CVF Conference on Computer Vision and Pattern Recognition*, 2022, pp. 14084–14093.

[27] Z. Wang, Z. Zhang, C.-Y. Lee, H. Zhang, R. Sun, X. Ren, G. Su, V. Perot, J. Dy, and T. Pfister, “Learning to prompt for continual learning,” in *Proceedings of the IEEE/CVF Conference on Computer Vision and Pattern Recognition*, 2022, pp. 139–149.

[28] X. Sun, P. Hu, and K. Saenko, “Dualcoop: Fast adaptation to multi-label recognition with limited annotations,” *arXiv preprint arXiv:2206.09541*, 2022.

[29] R. Zhang, W. Zhang, R. Fang, P. Gao, K. Li, J. Dai, Y. Qiao, and H. Li, “Tip-adapter: Training-free adaption of clip for few-shot classification,” in *European Conference on Computer Vision*. Springer, 2022, pp. 493–510.

[30] Y. Yao, A. Zhang, Z. Zhang, Z. Liu, T.-S. Chua, and M. Sun, “Cpt: Colorful prompt tuning for pre-trained vision-language models,” *arXiv preprint arXiv:2109.11797*, 2021.

[31] M. Jia, L. Tang, B.-C. Chen, C. Cardie, S. Belongie, B. Hariharan, and S.-N. Lim, “Visual prompt tuning,” in *European Conference on Computer Vision (ECCV)*, 2022.

[32] Y. Zhang, K. Zhou, and Z. Liu, “Neural prompt search,” *arXiv preprint arXiv:2206.04673*, 2022.

[33] P. W. Koh, S. Sagawa, H. Marklund, S. M. Xie, M. Zhang, A. Balsubramani, W. Hu, M. Yasunaga, R. L. Phillips, I. Gao *et al.*, “Wilds: A benchmark of in-the-wild distribution shifts,” in *International Conference on Machine Learning*. PMLR, 2021, pp. 5637–5664.

[34] C. Geng, S.-j. Huang, and S. Chen, “Recent advances in open set recognition: A survey,” *IEEE transactions on pattern analysis and machine intelligence*, vol. 43, no. 10, pp. 3614–3631, 2020.

[35] J. Wang, C. Lan, C. Liu, Y. Ouyang, T. Qin, W. Lu, Y. Chen, W. Zeng, and P. Yu, “Generalizing to unseen domains: A survey on domain generalization,” *IEEE Transactions on Knowledge and Data Engineering*, 2022.

[36] K. Zhou, Z. Liu, Y. Qiao, T. Xiang, and C. C. Loy, “Domain generalization: A survey,” *IEEE Transactions on Pattern Analysis and Machine Intelligence*, 2022.

[37] Y. Wang, L. Qi, Y. Shi, and Y. Gao, “Feature-based style randomization for domain generalization,” *IEEE Transactions on Circuits and Systems for Video Technology*, 2022.

[38] S. Yang, L. Liu, and M. Xu, “Free lunch for few-shot learning: Distribution calibration,” in *International Conference on Learning Representations*, 2020.

[39] W. Jiang, K. Huang, J. Geng, and X. Deng, “Multi-scale metric learning for few-shot learning,” *IEEE Transactions on Circuits and Systems for Video Technology*, vol. 31, no. 3, pp. 1091–1102, 2020.

[40] M. Cheng, H. Wang, and Y. Long, “Meta-learning-based incremental few-shot object detection,” *IEEE Transactions on Circuits and Systems for Video Technology*, vol. 32, no. 4, pp. 2158–2169, 2021.

[41] K. He, X. Zhang, S. Ren, and J. Sun, “Deep residual learning for image recognition,” in *Proceedings of the IEEE conference on computer vision and pattern recognition*, 2016, pp. 770–778.

[42] L. Fei-Fei, R. Fergus, and P. Perona, “Learning generative visual models from few training examples: An incremental bayesian approach tested on 101 object categories,” in *2004 conference on computer vision and pattern recognition workshop*. IEEE, 2004, pp. 178–178.

[43] F. Santambrogio, “{Euclidean, metric, and Wasserstein} gradient flows: an overview,” *Bulletin of Mathematical Sciences*, vol. 7, no. 1, pp. 87–154, 2017.

[44] Q. Liu, “Stein variational gradient descent as gradient flow,” *Advances in neural information processing systems*, vol. 30, 2017.

[45] M. Arbel, A. Korba, A. Salim, and A. Gretton, “Maximum mean discrepancy gradient flow,” *Advances in Neural Information Processing Systems*, vol. 32, 2019.

[46] A. Liutkus, U. Simsekli, S. Majewski, A. Durmus, and F.-R. Stöter, “Sliced-wasserstein flows: Nonparametric generative modeling via optimal transport and diffusions,” in *International Conference on Machine Learning*. PMLR, 2019, pp. 4104–4113.

[47] T. Li, L. Tan, Z. Huang, Q. Tao, Y. Liu, and X. Huang, “Low dimensional trajectory hypothesis is true: Dnns can be trained in tiny subspaces,” *IEEE Transactions on Pattern Analysis and Machine Intelligence*, 2022.

[48] J. Lee, L. Xiao, S. Schoenholz, Y. Bahri, R. Novak, J. Sohl-Dickstein, and J. Pennington, “Wide neural networks of any depth evolve as linear models under gradient descent,” in *Advances in Neural Information Processing Systems*, vol. 32, 2019, pp. 8572–8583.

[49] B. W. Larsen, S. Fort, N. Becker, and S. Ganguli, “How many degrees of freedom do we need to train deep networks: a loss landscape perspective,” in *International Conference on Learning Representations*, 2022.

[50] J. Deng, W. Dong, R. Socher, L.-J. Li, K. Li, and L. Fei-Fei, “Imagenet: A large-scale hierarchical image database,” in *2009 IEEE conference on computer vision and pattern recognition*. Ieee, 2009, pp. 248–255.

[51] O. M. Parkhi, A. Vedaldi, A. Zisserman, and C. Jawahar, “Cats and dogs,” in *2012 IEEE conference on computer vision and pattern recognition*. IEEE, 2012, pp. 3498–3505.

[52] J. Krause, M. Stark, J. Deng, and L. Fei-Fei, “3d object representations for fine-grained categorization,” in *Proceedings of the IEEE international conference on computer vision workshops*, 2013, pp. 554–561.

[53] M.-E. Nilsback and A. Zisserman, “Automated flower classification over a large number of classes,” in *2008 Sixth Indian Conference on Computer Vision, Graphics & Image Processing*. IEEE, 2008, pp. 722–729.

[54] L. Bossard, M. Guillaumin, and L. V. Gool, “Food-101-mining discriminative components with random forests,” in *European conference on computer vision*. Springer, 2014, pp. 446–461.

[55] S. Maji, E. Rahtu, J. Kannala, M. Blaschko, and A. Vedaldi, “Fine-grained visual classification of aircraft,” *arXiv preprint arXiv:1306.5151*, 2013.

[56] J. Xiao, J. Hays, K. A. Ehinger, A. Oliva, and A. Torralba, “Sun database: Large-scale scene recognition from abbey to zoo,” in *2010 IEEE computer society conference on computer vision and pattern recognition*. IEEE, 2010, pp. 3485–3492.

[57] M. Cimpoi, S. Maji, I. Kokkinos, S. Mohamed, and A. Vedaldi, “Describing textures in the wild,” in *Proceedings of the IEEE conference on computer vision and pattern recognition*, 2014, pp. 3606–3613.

- [58] P. Helber, B. Bischke, A. Dengel, and D. Borth, “Eurosat: A novel dataset and deep learning benchmark for land use and land cover classification,” *IEEE Journal of Selected Topics in Applied Earth Observations and Remote Sensing*, vol. 12, no. 7, pp. 2217–2226, 2019.
- [59] K. Soomro, A. R. Zamir, and M. Shah, “Ucf101: A dataset of 101 human actions classes from videos in the wild,” *arXiv preprint arXiv:1212.0402*, 2012.
- [60] B. Recht, R. Roelofs, L. Schmidt, and V. Shankar, “Do imagenet classifiers generalize to imagenet?” in *International Conference on Machine Learning*. PMLR, 2019, pp. 5389–5400.
- [61] H. Wang, S. Ge, Z. Lipton, and E. P. Xing, “Learning robust global representations by penalizing local predictive power,” *Advances in Neural Information Processing Systems*, vol. 32, 2019.
- [62] D. Hendrycks, K. Zhao, S. Basart, J. Steinhardt, and D. Song, “Natural adversarial examples,” in *Proceedings of the IEEE/CVF Conference on Computer Vision and Pattern Recognition*, 2021, pp. 15 262–15 271.
- [63] D. Hendrycks, S. Basart, N. Mu, S. Kadavath, F. Wang, E. Dorundo, R. Desai, T. Zhu, S. Parajuli, M. Guo *et al.*, “The many faces of robustness: A critical analysis of out-of-distribution generalization,” in *Proceedings of the IEEE/CVF International Conference on Computer Vision*, 2021, pp. 8340–8349.
- [64] A. Gupta, P. Dollar, and R. Girshick, “Lvis: A dataset for large vocabulary instance segmentation,” in *Proceedings of the IEEE/CVF conference on computer vision and pattern recognition*, 2019, pp. 5356–5364.
- [65] K. He, G. Gkioxari, P. Dollár, and R. Girshick, “Mask r-cnn,” in *2017 IEEE International Conference on Computer Vision (ICCV)*, 2017, pp. 2980–2988.
- [66] H. Caesar, J. Uijlings, and V. Ferrari, “Coco-stuff: Thing and stuff classes in context,” in *Proceedings of the IEEE conference on computer vision and pattern recognition*, 2018, pp. 1209–1218.
- [67] B. Cheng, A. Schwing, and A. Kirillov, “Per-pixel classification is not all you need for semantic segmentation,” *Advances in Neural Information Processing Systems*, vol. 34, pp. 17 864–17 875, 2021.